A GIS-Based Assessment of Active Tectonics from Morphometric Parameters and Geomorphic Indices of Assam Region, India

Laxmi Gupta
Shiv Nadar University
Navdeep Agrawal
Shiv Nadar University
Jagabandhu Dixit (jagabandhu.dixit@snu.edu.in)
Shiv Nadar University https://orcid.org/0000-0002-5450-578X
Subashisa Dutta
Indian Institute of Technology Guwahati

Research Article

Keywords: Active tectonics, Assam region, Linear parameters, Areal parameters, Geomorphic indices, IRAT

Posted Date: October 25th, 2021

DOI: https://doi.org/10.21203/rs.3.rs-1012102/v1

Version of Record: A version of this preprint was published at Journal of Asian Earth Sciences: X on December 1st, 2022. See the published version at https://doi.org/10.1016/j.jaesx.2022.100115.

A GIS-Based Assessment of Active Tectonics from Morphometric Parameters and Geomorphic Indices of Assam Region, India

Laxmi Gupta[1], Navdeep Agrawal[1], Jagabandhu Dixit[1,*], Subashisa Dutta[2]

[1]Disaster Management Laboratory, Shiv Nadar University, Delhi NCR, Uttar Pradesh 201314, India.

[2]Department of Civil Engineering, Indian Institute of Technology Guwahati, Guwahati, Assam 781039, India.

E-mail address of authors: lg100@snu.edu.in (L.G.); na655@snu.edu.in (N.A.); jagabandhu.dixit@snu.edu.in (J.D.); subashisa@iitg.ac.in (S.D.)

[*]**Corresponding Author:** jagabandhu.dixit@snu.edu.in

ABSTRACT

Assam region lies in the tectonic region of eastern Himalayas and flood plains of River Brahmaputra. The landscape of Assam is formed by the complex integration of the vertical and horizontal movement of the earth's crust and the depositional and erosional process by a river. The frequency of seismic events results in the deformation of landforms and it highly influences the drainage pattern of the area. The analysis of tectonic or neotectonic activity with the help of morphometric parameters and geomorphic indices helps in the identification of hazard-prone areas of the basin. In the present study, the active tectonics of the Assam region is assessed using SRTM DEM data of 30 m resolution to derive linear and aerial morphometric parameters and eight geomorphic indices of the selected ten basins. The morphometric parameters and geomorphic indices namely, stream length gradient (*Sl*), valley floor width to

height ratio (*Vfh*), hypsometric curve, hypsometric integral (*Hi*), asymmetric factor (*Af*), basin shape index (*BS*), transverse topographic symmetry (*T*), basin elongation ratio (*BE*) and stream sinuosity (*SS*) are calculated for each basin. With the help of GIS, the indices are classified into three tectonic activity classes i.e., from higher to lower and the average of the classes are combined to generate an index of relative active tectonics (IRAT). The four classes of IRAT are defined for the study area as i) very high; Class 1 (1.57 – 1.80), ii) high; Class 2 (1.81 – 2.06), moderate; Class 3 (2.07 – 2.26) and low; Class 4 (2.27 – 2.30). Class 1 of IRAT corresponds to Basin 1 and 6 with a total area of about 47740 km^2, basin 2, 4 and 5 falls under Class 2 of IRAT and its total area is 2507 km^2, class 3 covers a total area of 17495 km^2 of basin 7,8 and 9 and Class 4 IRAT consists of basin 3 and 10 of total area 2090 km^2. Results show that the majority of the study area lies in very high to moderate active tectonic zones and these zones are consistent with the presence of major faults and thrusts of the basin area. It can be concluded that the combined approach of GIS-based morphometric and geomorphic study of a region allows in the identification of deformed landforms resulting from active tectonics.

Keywords: Active tectonics; Assam region; Linear parameters; Areal parameters; Geomorphic indices; IRAT

1. Introduction

Interaction of the Indian plate with the Eurasian plate led to the rise of the Himalayan which ranges from the North-East region (NER) of India to the Hindu Kush region (Afghanistan) in the west (Ghosh et al., 2018). The Indian plate is active and subducting under the Eurasian Plate at an average rate of 50 mm/year (Catherine, 2004) which makes the Himalayan belt one of the most seismo-tectonically active regions in the world. The active tectonic region undergoes changes that may either be gradual, fast, or rapid due to underneath tectonic activities. The formation of folds, faults, and basins is evidence of past deformation processes due to tectonic activity (Das et al., 2011). However, the gradual geomorphological

changes occurring in the region cannot be in the form of readily observable variations in surface deformations and basin drainage patterns and characteristics. These silent changes occurring in any region can be identified by morphotectonic and geomorphic analysis (Taesiri et al., 2020; Divyadarshini and Singh, 2019; Mishra, 2019). In active regions, the basin drainage pattern is sensitive to tectonic activity and processes like folding and faulting which results in drainage geometry, basin asymmetry, river deflection, and accelerated incision (Cox, 1994; Saber et al., 2020). These changes in the river system are also an efficient indicator of differential uplift due to active tectonics (Mishra, 2019).

The geomorphic indices such as hypsometric integral (Strahler, 1952; Daxberger et al., 2014), asymmetric factor (Hare and Gardner, 1985), basin shape (Bull and McFadden, 1977), the ratio of basin elongation (Bull and McFadden, 1977), the width of valley floor to valley height ratio (Bull and McFadden, 1977), index of stream length gradient (Hack, 1973), stream sinuosity (Mueller, 1968) and transverse topography symmetry (Cox, 1994) have been successfully used in active tectonic studies in the past by various researchers (Das et al., 2011; Mahmood and Gloaguen, 2012; Sharma and Sarma, 2017; Taesiri et al., 2020). Similarly, evaluation of morphometric parameters comprises of stream order and number, bifurcation ratio, the ratio of stream length, drainage density and texture, stream frequency of drainage, drainage texture, circularity ratio, and drainage form factor, are also used as indicators for the assessment of active tectonics of any region (Shukla et al., 2013; Topal 2018; Anand and Pradhan 2019; Bahrami et al., 2020).

Remote sensing and GIS play an important role in data collection and spatial analysis for these indices (Sarp and Duzgun, 2015; Koukouvelas et al., 2018; Alizadeh et al., 2020). This approach is less time-consuming and eliminates the chances of possible errors in data collection by conventional methods of field surveys. In the present study, morphometric and geomorphic indices were extracted from DEM (digital elevation model) for the state of Assam,

NER India, and quantitatively analyzed to evaluate the gradual changes of the basin area due to active tectonics. Assam lies in the foothills of the north-eastern Himalayan and the flood plains of Brahmaputra River, one of the largest anabranching mega-rivers in the world (Latrubesse, 2008). The region of Assam has high seismicity with complex tectonic and geological settings (Fig. 1a).

The western portion of Assam is sandwiched between the MFT and Dauki Fault (forming Shillong Plateau in the south of the study area) while the eastern portion is sandwiched between MFT and Naga thrust with Mishmi thrust trending NW-SE in the NE which led to the formation of flood plains of alluvial deposits from east to west except for the central part of the state (Fig. 1b). The central part also comprises major faults like the Kopili fault and Dighalpani-Kakijan fault with extensions of the Dauki fault and Naga thrust, forming the separate drainage basin of several rivers other than the Brahmaputra River basin (Panda et al., 2018; Bahuguna and Sil, 2020).

In the past, this region has experienced many significant earthquakes as high as Mw 8 due to the activity of these tectonic features. The continuous activity of tectonic and movement has affected the morphology of the Himalayan foreland (Devi, 2007; Raghukanth et al., 2011; Dixit et al., 2016; Biswas and Paul, 2021). Therefore, an attempt was made to evaluate the tectonic activity of the entire state of Assam based on morphometric and geomorphic indices using remote sensing data and a GIS-based approach. Similar approaches have been successfully used in other active tectonic regions such as Nagaland India (Longkumer et al., 2018), Hindu Kush Afghanistan (Mahmood and Glaoguen, 2011), Siwalik Hills of Himalayans (Singh and Chaudhri, 2020), Qianhe river basin North China (Zhang et al., 2019), Greater Antilles North America (Rodriguez et al., 2017), Coasts of Mediterranean Sea Spain (Silva et al., 2003) and NW Iran (Saber et al., 2018).

In the present study, we use eight geomorphic indices and seven morphometric indices. The methodology and evaluation of these indices are discussed in detail in the following sections.

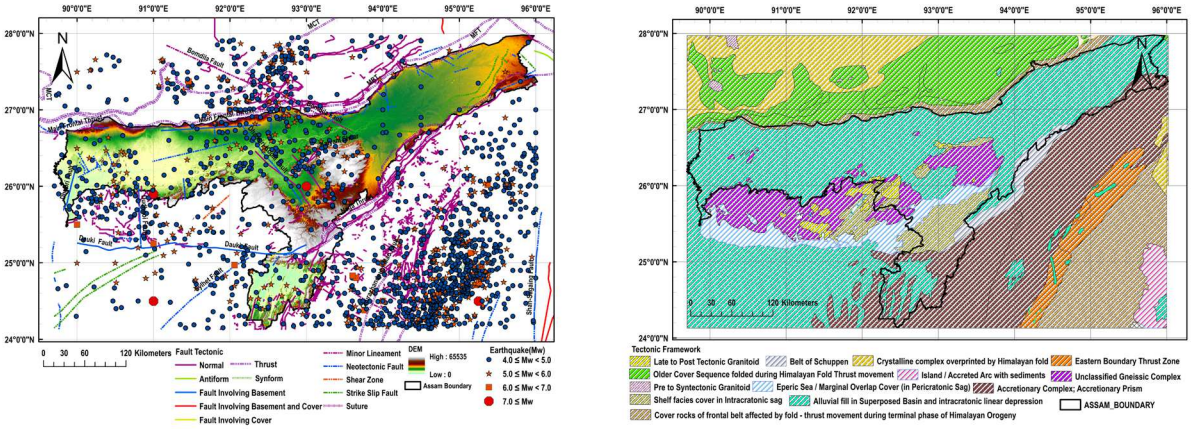

(a) (b)

Fig. 1. Map of the study area and its surroundings showing (a) major fault tectonics, seismicity, and elevation, and (b) geotectonic framework.

2. Methodology

The present study aims at GIS (Geographic Information System) based determination of morphometric parameters and geomorphic indices to assess the tectonic activity of the Assam region. The study area consists of Brahmaputra valley and Barak valley and it is further divided into 10 basins of stream order varies from 1st to 7th order (Strahler, 1957). For the present study, the basin having a stream equal to and greater than 3 is considered for the quantification of morphometric parameters and geomorphic indices. The morphometric parameters (linear and areal parameters) and geomorphic indices are extracted with the help of 1 arc second Shuttle Radar Topography Digital Elevation Model (SRTM DEM) data of 30m resolution (https://earthexplorer.usgs.gov/), earthquake data (Bhukosh-Geological Survey of India; United States Geological Survey; International Seismological Centre) and tectonic framework of the study area (Bhukosh-Geological Survey of India). With the help of the DEM layer with 30 m resolution, two primary layers i.e., watershed and river vector layers are

extracted by GIS ModelBuilder in ArcGIS 10.5 software as shown in Fig. 2 (Ilalahia and Hidayatb, 2019; Dawit et al., 2020; Khan et al., 2021). The watershed and river layer are further applied for the calculation of morphometric indices consisting of two linear and five areal parameters and eight geomorphic indices and for each index a raster layer is generated.

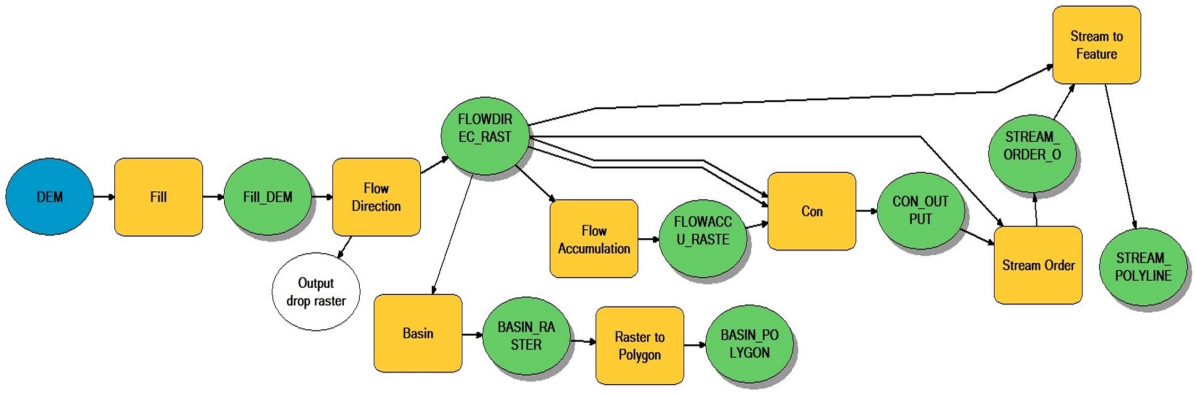

Fig. 2. GIS model for the extraction of basins and streams using DEM data.

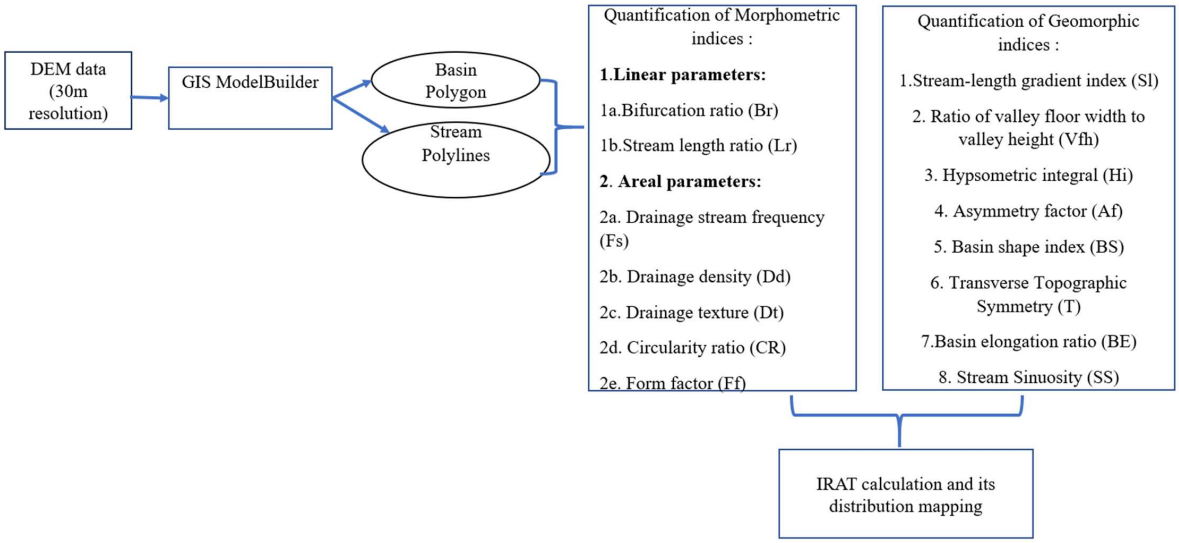

Fig. 3. Schematic diagram of the methodology adopted in the study.

Each layer is classified into three classes based on their tectonic activity and finally, IRAT (Indices of relative active tectonics) is calculated to identify the tectonically active region with the help of morphotectonic indices (Cheng et al., 2016; Gu et al., 2019; Bhattacharjee and

Mohanty, 2020; Pei et al., 2021). The flowchart of the adopted methodology is illustrated in the schematic diagram in Fig. 3 and details of different morphometric and geomorphic indices are presented in the upcoming section of this study.

3. Evaluation of Indices

Morphometric and geomorphic indices can be defined as a tool that helps in the determination of deformational process as well as the evolution of a landform due to dynamic processes (Raj, 2012; Bhat et al., 2020). These indices act as an indicator of anomalies in the drainage system that arises due to tectonic activity and thus differentiate tectonically active zones of the region. In the present study, 10 basins of the Assam region are delineated and morphometric and geomorphic indices are evaluated for each basin. Each index is categorized into three tectonic classes based upon the range of values. The schematic representation of the parameters of geomorphic indices is shown in Fig. 4.

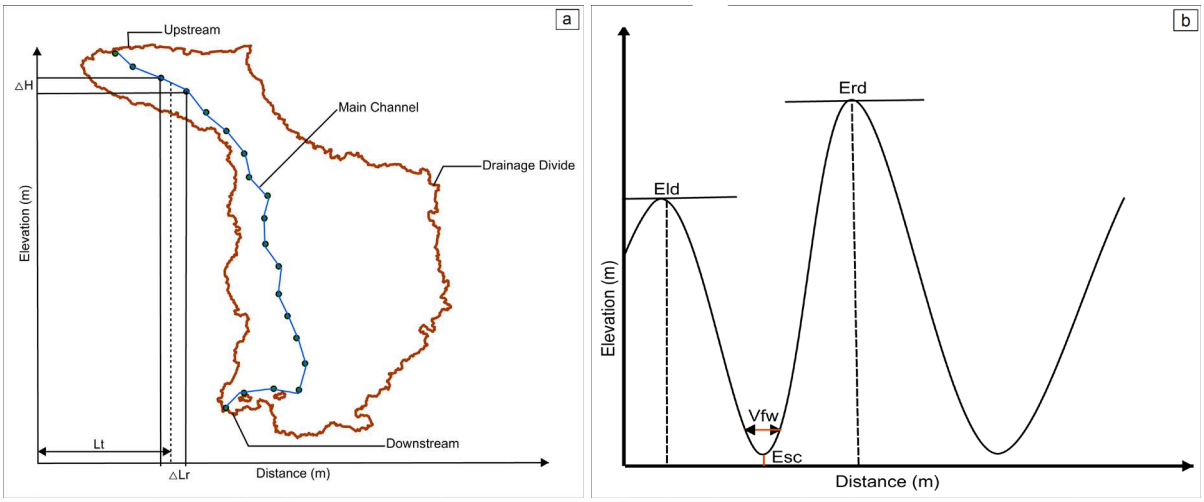

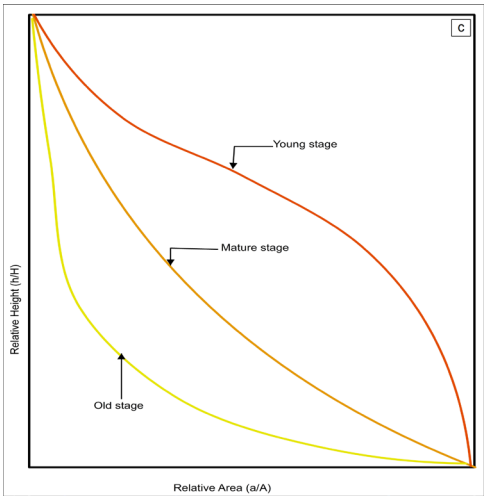
c
Young stage
Mature stage
Old stage
Relative Height (h/H)
Relative Area (a/A)

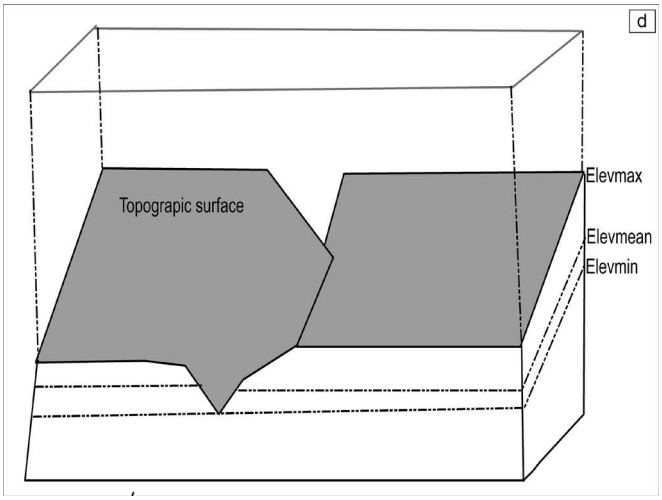
d
Topograpic surface
Elevmax
Elevmean
Elevmin

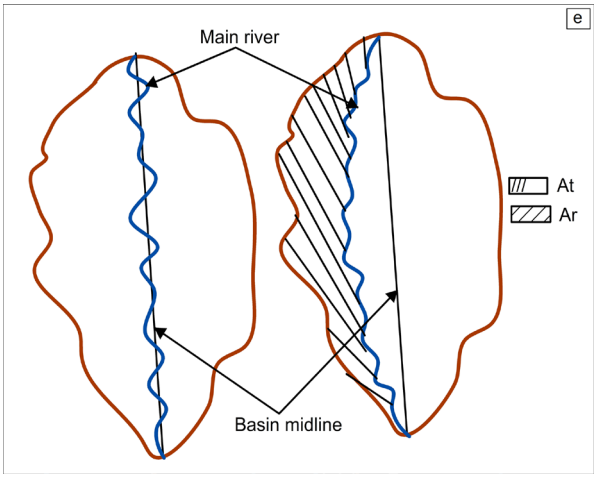
e
Main river
At
Ar
Basin midline

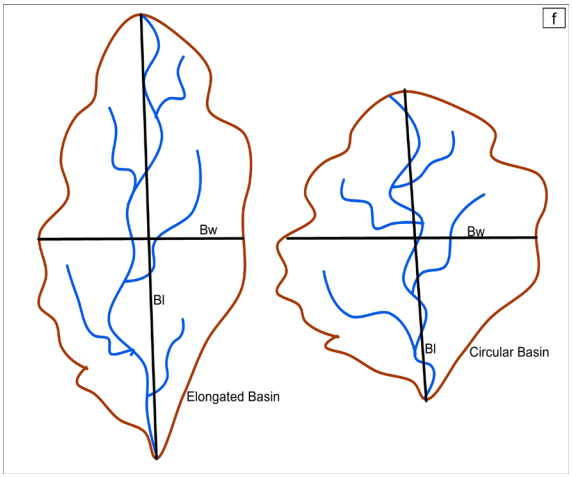
f
Bw
Bl
Elongated Basin
Bw
Bl
Circular Basin

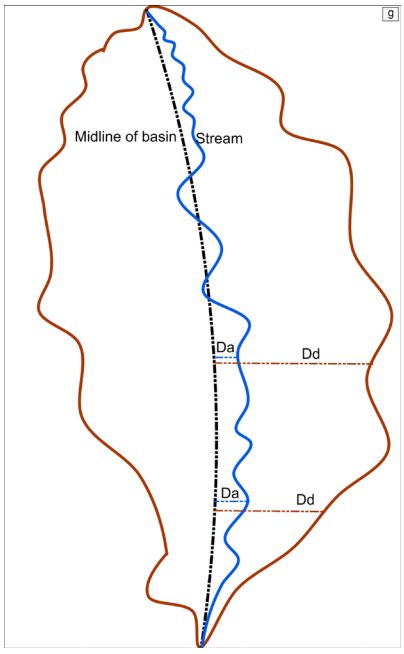
g
Midline of basin
Stream
Da
Dd
Da
Dd

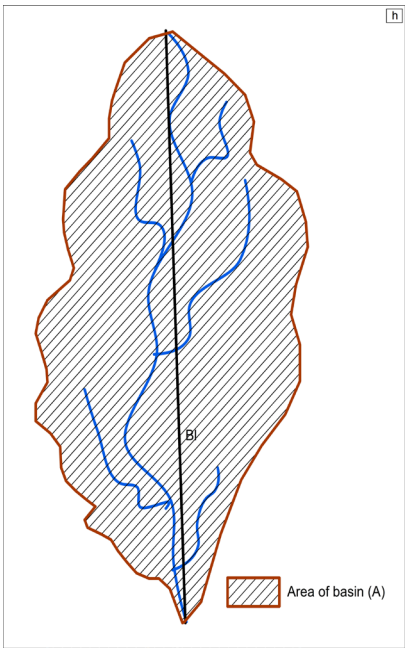
h
Bl
Area of basin (A)

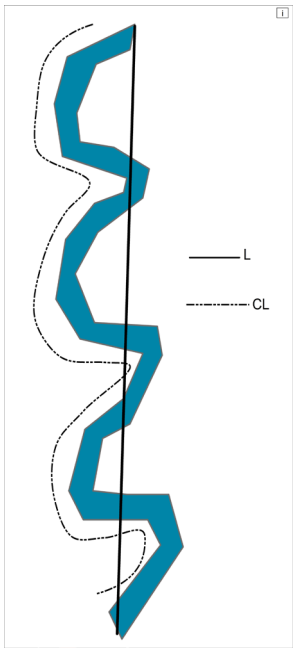
i
L
CL

Fig. 4. Parameters of Geomorphic Indices (a) Stream length gradient (*Sl*), (b) Valley floor width to height ratio (*Vfh*), (c) Hypsometric curve, (d) Hypsometric integral (Hi), (e) Asymmetric factor (*Af*), (f) Basin shape index (*BS*), (g) Transverse topographic symmetry (*T*), (h) Basin elongation ratio (*BE*), (i) Stream sinuosity (*SS*).

Finally, the index of relative active tectonics (IRAT) is calculated and classified into four tectonic activity classes for the entire region by taking the arithmetic mean of morphometric and geomorphic indices classes.

3.1. Morphometric Indices

3.1.1. Linear parameters

The linear parameters are used to evaluate the evolution one dimensional characteristic of the drainage basin. In the present study, the linear parameters considered are Stream order (*U*), stream number (*Nu*), bifurcation ratio (*Br*), and stream length ratio (*Lr*). Among the four linear parameters, the bifurcation ratio (*Br*) and stream length ratio (*Lr*) are the most significant ones. The highest stream order of the basin is of seventh order, the stream order of each basin is calculated (Table 1 and Fig. 5)

The Bifurcation ratio is calculated by the equation

$$Br = \frac{N_u}{N_{u+1}} \quad (1)$$

N_u is the number of streams of a particular order and N_{u+1} is the number of streams of higher-order (Horton, 1945). The high values of B_r represent a young stage of the basin and low values signify the mature development stage of the basin.

The range of *Br* values in the present study varies between 1.25 (Basin 7) and 3.58 (Basin 5). The calculated values are divided into three classes (Anand and Pradhan, 2019): Class 1(3.58 – 2.32), Class 2 (2.31 – 2.00), and Class 3 (< 2.00).

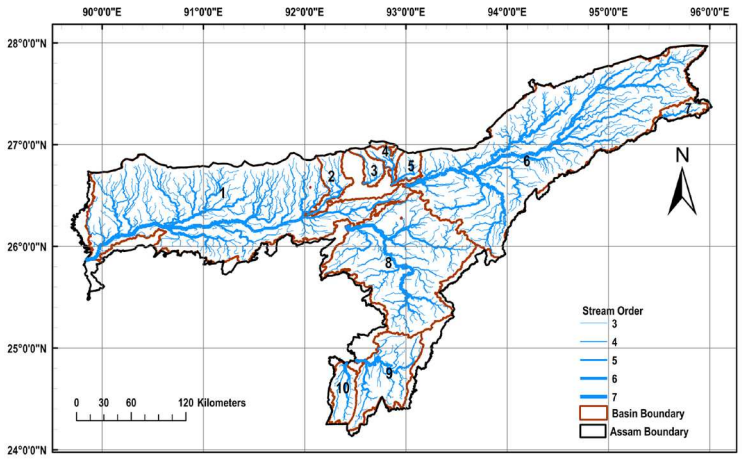

Fig. 5. Stream order of the basins.

Stream length ratio (*Lr*) is defined as the linear parameter of a basin and it is expressed as the ratio of the total length of a stream of specific higher stream order to the total length of stream of next lower order as given by the equation,

$$Lr = \frac{L_u}{L_{u-1}} \quad (2)$$

L_u is the total length of particular stream order and L_{u-1} is the total stream length of the lower order (Sreedevi et al., 2005). The value of *Lr* of a basin depends on the prevailing slope and topographic conditions. The surface flow discharge and erosional stage of the basin are also defined by the stream length ratio. In the present study, the minimum value of *Lr* is 0.48 (Basin 8) and 2.14 (Basin 5), and the classification of Lr are as follows (Anand and Pradhan, 2019): Class 1 (2.14 – 1.11), Class 2 (1.12 – 0.55), and Class 3 (< 0.55).

After the classification of values into three tectonic activity classes i.e., Class 1 (high), Class 2 (moderate), and Class 3 (low) for the two linear parameters (Table 1), the average class value of the two linear parameters is taken and divided into three classes of tectonic activity as Class 1, 2 and 3 (Table 3 and Fig. 10a).

3.1.2. Areal parameters

171 The areal parameters of a basin mainly include drainage density (D_d), drainage Stream
172 frequency (F_s), drainage texture (D_t), circularity ratio (CR), and form factor (F_f). In the present
173 study, the above-mentioned areal parameters are evaluated for the analysis of erosional
174 processes taking place in the basin.

175 The drainage density (D_d) of the basin can be explained mathematically as:

176 $$Dd = \frac{\sum L_t}{A} \quad (3)$$

177 where L_t denotes the length of the total stream and A is the total area of the basin
178 (Horton, 1945). The factor D_d depends on the geological condition, rainfall intensity, type of
179 soil, and vegetation (Horton, 1945). The minimum and maximum value of drainage density in
180 the study are 0.19 (Basin 10) and 0.23 (Basin 1) respectively and the classes are (Anand and
181 Pradhan, 2019): Class 1(0.23 – 0.208), Class 2 (0.207 – 0.20) and Class 3 (< 0.200).

182 Drainage Stream frequency (F_s) is calculated for each basin with the help of equation

183 $$Fs = \frac{\sum N_u}{A} \quad (4)$$

184 N_u is the sum of segments of stream of all orders in the basin and A represents the total
185 area of the basin (Horton, 1945). The range of F_s lies between 0.131 to 0.169 for Basin 3 and
186 Basin 10 respectively. To determine the tectonic activity class of each basin, the values
187 obtained in the study are grouped into high, moderate, and low classes as 0.169 – 0.145 (Class
188 1), 0.144 – 0.140 (Class 2), and < 0.140 (Class 3) respectively.

189 The drainage texture (D_t) of a basin can be defined by the equation

190 $$Dt = \frac{\sum N_u}{P} \quad (5)$$

where N_u equals the sum of stream segments of all orders in the basin and P is the perimeter of the basin (Horton, 1945). The range of D_t calculated for the ten basins varies from 0.354 (Basin 4) to 2.638 (Basin 6) and the classification of the D_t values are: Class 1(2.638 – 2.109), Class 2 (2.108 – 0.536), and Class 3 (< 0.536).

The parameters D_d, F_s, and D_t indicate the permeability, relief, and infiltration capacity of a basin. If the values of D_d, F_s, and D_t are high, it implies low infiltration capacity, impermeability, and high relief conditions whereas lower values indicate high infiltration rate, permeable lithological conditions, and presence of lower relief (Shukla et al., 2013).

The circularity ratio (CR) and form factor (F_f) is the areal parameters of a basin evaluated for the identification of the shape of the drainage basin. The circularity ratio (CR) of the basin is calculated by the equation

$$CR = \frac{4\pi A}{P^2} \tag{6}$$

Where A and P represent the area and perimeter of the basin respectively. The circulatory ratio (CR) is influenced by the geology, slope, and land cover of the selected area. The circulatory ratio (CR) calculated in this study lies from 0.122 (Basin 4) to 0.301 (Basin 10). The values of CR are classified into three different active tectonic classes (Anand and Pradhan, 2019): Class 1(0.122 – 0.207), Class 2 (0.208 – 0.264), and Class 3 (0.265 – 0.301) correspond to high, low, and moderate respectively. The high value of CR denotes a circular basin that tends to evolve into an elongated basin.

The form factor (F_f) can be expressed by the given equation

$$Ff = \frac{A}{L_b^{\,2}} \tag{7}$$

The term A defines the basin area and L_b is the length of the basin. For the present study, the value of F_f ranges from 0.178 (Basin 2) to 0.364 (Basin 8) and the values are further grouped into high to low tectonic classes as (0.178 – 0.207), (0.208 – 0.330), and (> 0.330) belongs to Class 1, Class 2 and Class 3, respectively (Anand and Pradhan, 2019). The low form factor values mainly describe the elongated basins which are structurally and tectonically controlled.

Each of the areal parameters is classified into three classes as Class 1(high), Class 2 (moderate), and Class 3 (low) as per the tectonic activity (Table 1) and their average values of class are determined and categorized into high, medium and low class represented as Class 1, Class 2 and Class 3 respectively (Table 3 and Fig. 10b).

Table 1 Morphometric Indices parameters.

Basin no		Linear Parameters		Areal Parameters				
	U	*Br*	*Lr*	*Fs*	*Dd*	*Dt*	*CR*	*Ff*
1	7	2.19	0.55	0.14	0.23	2.11	0.12	0.19
2	5	1.59	0.72	0.14	0.22	0.48	0.13	0.18
3	5	2.11	0.53	0.13	0.21	0.44	0.21	0.35
4	5	1.30	1.11	0.14	0.20	0.35	0.12	0.33
5	5	3.58	2.14	0.14	0.20	0.54	0.27	0.36
6	7	2.00	0.50	0.14	0.21	2.64	0.17	0.21
7	5	1.25	0.76	0.15	0.19	0.53	0.27	0.27
8	7	2.32	0.48	0.14	0.19	1.98	0.21	0.36
9	6	2.44	0.52	0.14	0.20	1.23	0.22	0.29
10	6	1.45	0.56	0.17	0.19	0.99	0.30	0.35

3.2. Geomorphic Indices

3.2.1. Stream-length gradient index (Sl)

When the river and streams flow through their course, a dynamic equilibrium is reached when erosional processes equal the upliftment of landmass and as a result, the river system tends to form a concave longitudinal profile (Hack, 1973; Schumm et al., 2000). This stable profile of the river system tends to deviate due to various factors mainly lithological, climatic, or tectonic. To evaluate the influence of environmental factors on the longitudinal profile of the river and streams, *Sl* index can be calculated. It is a quantitative approach that is based on the depositional and erosional processes of a drainage system and also determines the reach of equilibrium by the streams. It is found that the *Sl* index is used in the evaluation of the tectonic activity of a region, an area with soft rocks having high *Sl* values indicates the occurrence of recent tectonic activity, and high *Sl* values also represent the presence of river flow through the strike-slip faults. Mathematically *Sl* index can be defined as

$$Sl = \left(\frac{\Delta H}{\Delta L_r} \right) * L_t \tag{8}$$

$\triangle H$ is the elevation change, $\triangle L_r$ is the length of the reach and L_t is the horizontal distance from the divide of the watershed reach midpoint (Fig. 4a).

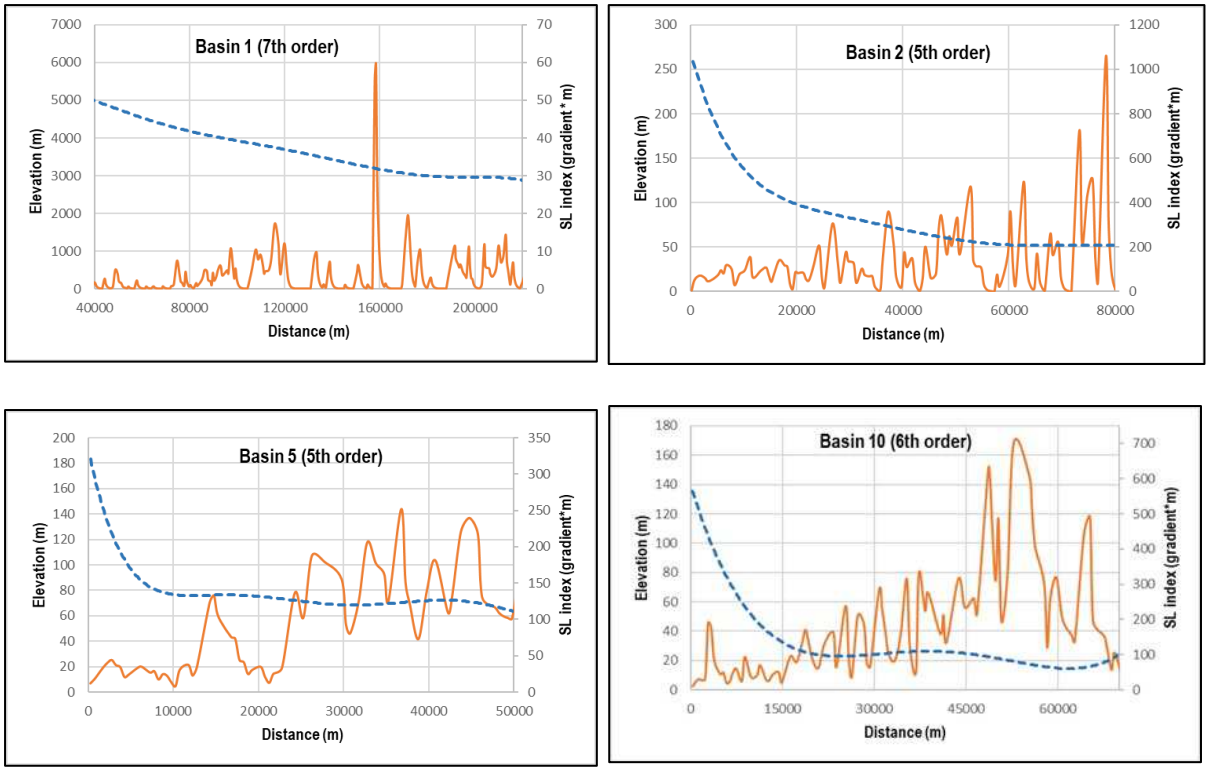

Fig. 6. Longitudinal River profile (*LP*) and Stream Length Gradient index (*Sl*) of selected basins.

In this study, the value of *Sl* is calculated along the river and stream length (Fig. 6), and the standardized values are estimated for the classification. The range of *Sl* values for the 10 basin lies between 62.58 (Basin 4) to 466.87 (Basin 9) and classified into three classes (Mahmood and Gloaguen, 2012), in Fig. 10c, as Class 1 (> 250), Class 2 (250 – 120) and Class 3 (< 120).

3.2.2. Valley floor width to valley height ratio (Vfh)

Valley floor width valley height ratio (*Vfh*) is one of the important geomorphic indices which is used for the discrimination between V-shaped and U-shaped valleys and also gives a representation of active tectonics of a region (Bull and McFadden, 1977). Mathematically the index can be defined as:

$$Vfh = \frac{2Vf_w}{\left(E_{rd} - E_{sc}\right) + \left(E_{ld} - E_{sc}\right)} \quad (9)$$

where Vf_w is the valley floor width, E_{sc} is the average elevation of the valley floor, E_{rd} and E_{ld} are the elevations of the right and left valley divide facing in the downstream direction respectively (Fig. 4b).

The *Vfh* index gives an indication of incision and uplift along a river channel. The low value of *Vfh* signifies a higher incision and uplift rate resulting in deep V-shaped valleys due to the dominance of tectonic activity over erosional processes. The high value of *Vfh* corresponds to a U-shaped valley or flat-floored valleys mainly formed due to erosional processes at bed level. For the present study, cross-sections are drawn from the DEM data at a given distance, and the cross-sections are shown in (Fig. 7).

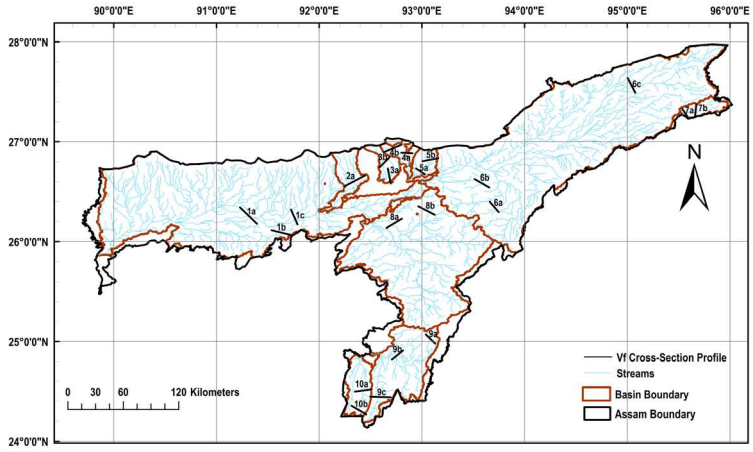

Fig. 7. Cross-sections for calculation of the ratio of Valley floor width to height (*Vfh*).

The average value of *Vfh* is calculated for the basins where more than one cross-section is drawn and the average values are divided into three active tectonic class Class 1 (0.260-0.660), Class 2 (0.661-0.900), and Class 3 (> 0.900) describing the high, medium and low tectonic activity of the basins, respectively (Mahmood and Gloaguen, 2012). The results indicate that the lowest value of *Vfh* is 0.260 for basin 7 and the highest value is 8.540 for basin 1, which describes that shape of basin 1 and basin 7 are comprised of U- and V-shaped valleys

respectively. For basins 2,4,5,7 and 10, the value of *Vfh* is less than 1 and the values are more than 1 for basins 1,3,6,8, and 9 (Fig. 10d).

3.2.3. Hypsometric integral (Hi) and hypsometric curve

Hypsometric integral and hypsometric curves explain the erosional and depositional processes occurring in a drainage basin that is linked with the tectonic evolution and geomorphology of the basin. The *Hi* index is defined as the elevation distribution of a given area of the drainage basin and it is represented by the area that lies below the hypsometric curve expressing the total volume of the non-eroded basin.

Hypsometric curves are graphical representation which is obtained by plotting the proportion of total elevation of basin against the proportion of total basin area (Fig. 8). Based on the shape of the hypsometric curve, the stages of the basin can be classified as (i) concave curve signifies old eroded basin region, (ii) S-shaped curve denotes basin regions that are moderately eroded, and (iii) convex hypsometric curve represent a young stage of the basin that are slightly eroded (Fig. 4c) (Strahler, 1952). The values of *Hi* ranges from 0 to 1 and can be calculated as:

$$Hi = \frac{\left(Elev_{mean} - Elev_{min}\right)}{\left(Elev_{\max} - Elev_{min}\right)} \quad (10)$$

$Elev_{mean}$, $Elev_{min,}$ and $Elev_{max}$ are the mean, minimum and maximum elevation of the basin respectively (Fig. 4d).

For the calculation of *Hi*, Daxberger's methodology is adopted using ArcGIS 10.5 (Daxberger et al., 2014). The high *Hi* value is an indication of a younger landscape that is formed due to recent tectonic activity whereas low *Hi* value is related to older landforms that are more eroded but less affected by tectonic activity recently.

The result of *Hi* for the 10 basins are grouped into three classes (Mahmood and Gloaguen, 2012): Class 1 (0.200 – 0.287), Class 2 (0.100 – 0.199), and Class 3 (< 0.100)

defining high, moderate, and low tectonic active class respectively (Fig. 10e). The value of *Hi* is lowest for basin 9 (0.020) and highest for basin 4 (0.287).

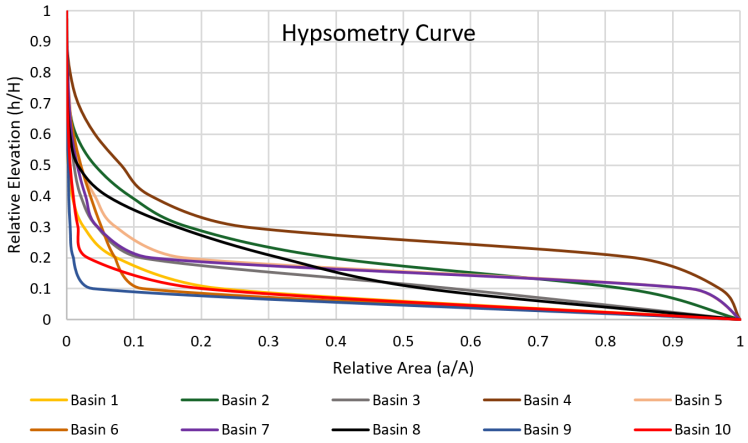

Fig. 8. The hypsometric curve of 10 basins of the study area.

3.2.4. Asymmetric Factor (Af)

Asymmetry factor (*Af*) is an essential parameter of basin drainage and determines the existence of tectonic tilting of the basin. The tilting in the basin arises due to the tectonic disturbance and it causes deviation of the main river channel from the midline of the basin to the direction in which tilting has occurred. It can be applied at basin drainage scale as well as over a large area and mathematically it can be expressed as

$$Af = \left(\frac{A_r}{A_t} \right) * 100 \tag{11}$$

A_r denotes the basin area to the right of the mainstream in the downstream direction and the total area of the basin is A_t (Fig. 4e) (Hare and Gardner, 1985). The value of *Af* greater than or smaller than 50 indicated the presence of tectonic activity or lithological control and *Af* close to 50 signifies that no or less tilting is present. Before the calculation of the *Af* parameter for the 10 basins of the study area, the thalweg line is drawn for each basin and the area on both sides of the thalweg line is determined in the GIS environment. The tilting direction of the basin is identified (Fig. 9) and the descriptive value of *Af* is considered equal to the absolute value of (*Af*-50).

The range of *Af*-50 is between 0.144 (Basin 5) and 26.678 (Basin 3) denoting almost symmetric and highly unsymmetric basins, respectively. The values of *Af* obtained in the study are classified into three classes (Mahmood and Gloaguen, 2012) as in Fig. 10f: Class 1 (17.831-26.678), Class 2 (8.981-17.830), and Class 3 (< 8.981).

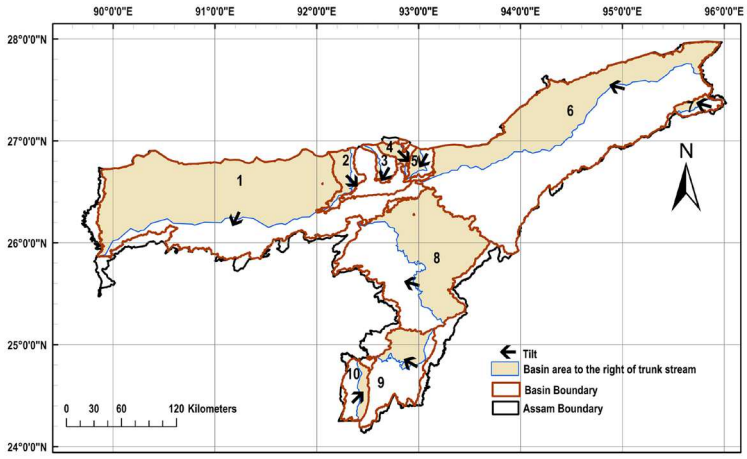

Fig. 9. The direction of the titling of basins in the study area.

3.2.5. Drainage Basin shape index (Bs)

In an active tectonic area, the basin exhibits an elongated shape and it tends to attain a circular shape with topographic evolution or decreasing of tectonic activity (Bull and McFadden, 1977). This transformation takes place because in an active tectonic area the width of the drainage basin is narrow near the mountain front and the energy of the stream is primarily directed in the direction of downcutting. In contrast, the areas that lack the continuing rapid uplift favor the widening of the drainage basin upstream of the mountain front (Ramírez-Herrera, 1998). The basin shape index can be expressed as

$$Bs = \frac{B_l}{B_w} \tag{12}$$

where B_l defines the total distance measured from the source to the mouth of the basin and B_w is the maximum measured width of the basin (Fig. 4f).

The elongated basins have high *Bs* values and it is related to higher tectonic activity and the circular basins having very low tectonic activity exhibit low *Bs* value. So, the values

of *Bs* can be used as an indicator of the rate of tectonic activity of a basin. In the present study, *Bs* are calculated using the DEM data and the results are classified (Taesiri et al., 2020) into Class 1 (2.450 -3.080); Class 2 (1.830 – 2.449), and Class 3 (< 1.830) denoting high, moderate, and low active tectonics of the basins respectively. The range of *Bs* values lies between 1.210 (Basin 8) to 3.080 (Basin 1) and spatially distributed (Fig. 10g).

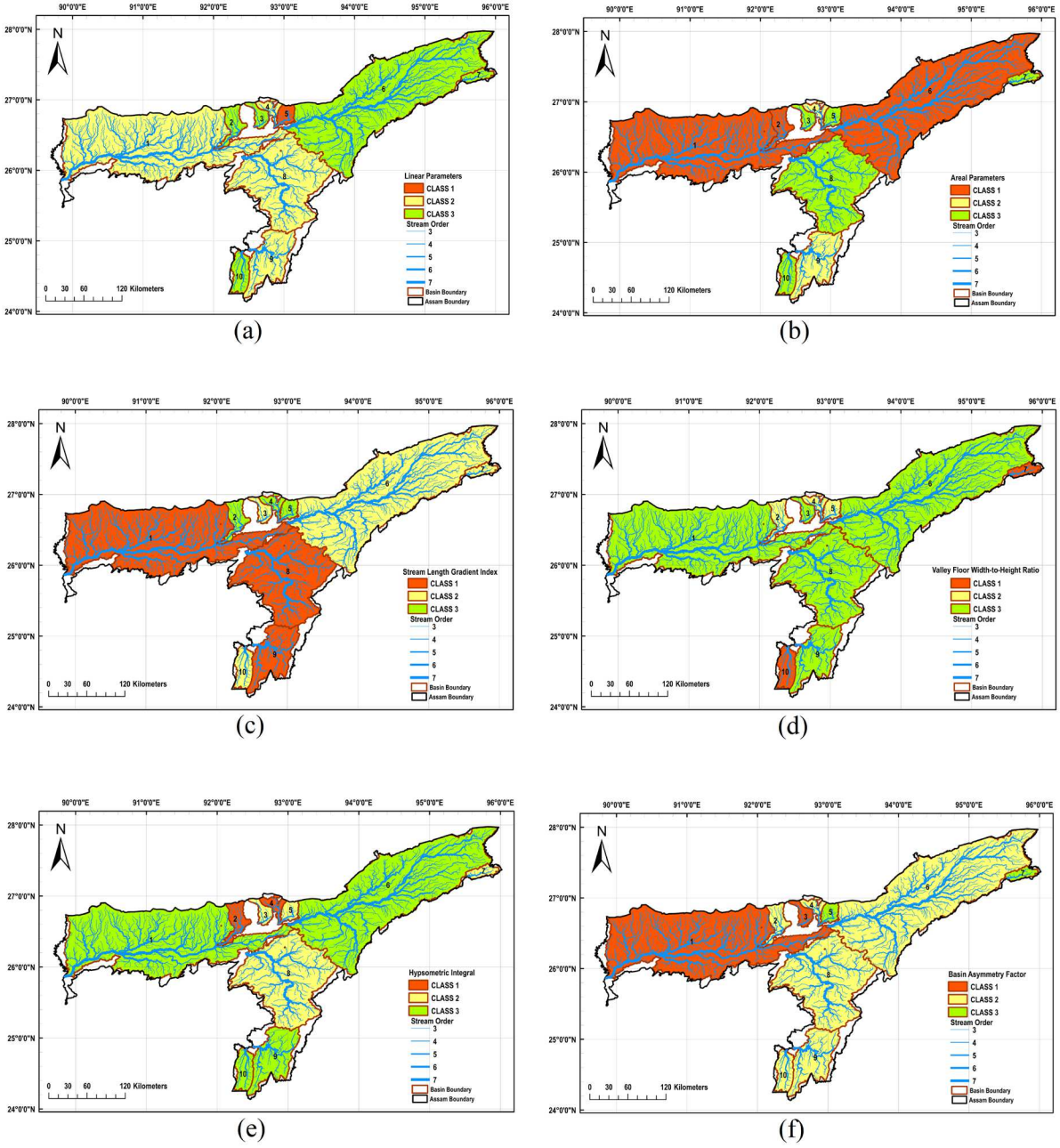

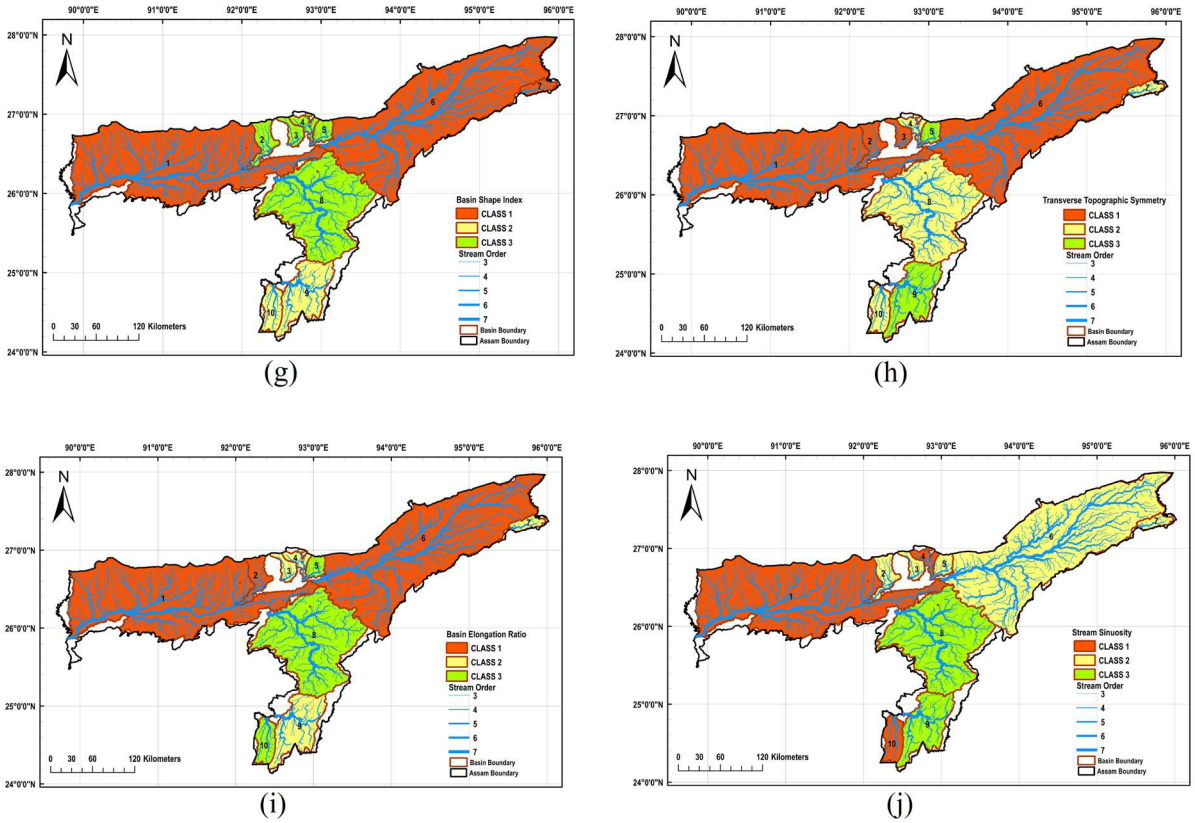

Fig. 10. Spatial distribution of (a) Linear parameters (b) Areal parameters (c) Stream length gradient (*Sl*), (d) Valley floor width to height ratio (*Vfh*), (e) Hypsometric integral (Hi), (f) Asymmetric factor (*Af*), (g) Basin shape index (*BS*), (h) Transverse topographic symmetry, (i) Basin elongation ratio (*BE*), (j) Stream sinuosity (*SS*).

3.2.6. Transverse topographic symmetry (T)

The transverse topographic symmetry (*T*) is calculated for measuring the tilting of the basin due to the presence of tectonic activity. *T* index is calculated based on the symmetry vector data of the basin which includes deflection of the meander belt from the midline of the basin. The value of *T* can be calculated by the given equation and it ranges from 0 to 1.

$$T = \frac{D_a}{D_d} \tag{13}$$

In the above equation, D_a is defined as the deflection of the channel of the stream from the basin midline and D_d is the distance between basin midline and basin divide (Fig. 4g).

In the present study, *T* is calculated at a distance interval of 500 meters for every 10 basins and symmetric basin *T*= 0 and asymmetric basin *T*> 0 (Cox, 1994). The minimum value of *T* obtained in the present study is 0.080 for Basin 5 and the maximum value of *T* is 0.540 for Basin 3. The *T* values are classified into three classes (Taesiri et al., 2020) as follows Class 1 (0.380-0.540), Class 2 (0.230 – 0.379) and Class 3 (< 0.230) from high to low tectonic activity (Fig. 10h).

3.2.7. Basin elongation ratio (BE)

Basin elongation ratio is a significant geomorphic index that supports the neotectonic activity of a drainage basin. It is a dimensionless quantity, determined as the ratio of the diameter of a circle which has an equal area as the of the basin under consideration and the maximum basin length (Bull and McFadden, 1977). The area of each basin and its maximum length is calculated in the ArcGIS 10.5 and the value of BE is calculated by the given expression,

$$BE = \frac{2(A/\pi)^{0.5}}{B_l} \tag{14}$$

where A and B_l are the area and maximum length of the basin, respectively (Fig. 4h).

The basin areas having the value of *BE* below 0.50 are tectonically active areas, between 0.50 to 0.75 are considered as slightly active and more than 0.75 falls under inactive tectonic area. The lowest and highest value of *BE* obtained in the study is 0.477 and 0.684 suggesting that the study area of the basins falls under tectonically active to a slightly active class. The values of BE obtained in the present study are divided into three classes (Mahmood and Gloaguen, 2012) of high, moderate, and low tectonic activity as Class 1 (0.477 – 0.502), Class 2 (0.503 – 0.664), and Class 3 (0.665 – 0.684), respectively (Fig. 10i).

3.2.8. Stream Sinuosity (SS)

In the assessment of the tectonic activity of an area, stream sinuosity can also be considered as an important indicator. The index of stream sinuosity can be obtained by the ratio of the length of a stream i.e., the curvilinear path and length of the straight line joining the two ends of the selected channel reach. Mathematically, it can be written as,

$$SS = \frac{CL}{L} \tag{15}$$

where, CL = Length of stream channel and L = Straight line joining the two ends of the channel (Fig. 4i).

If the value of *SS* is high, it indicates that the river is tectonically stable and it is closer to equilibrium whereas a low value of *SS* denotes that the basin area is active (Mueller 1968). The value of $SS < 1.05$ represent tectonic active, $1.05 < SS < 1.5$ are semi-active and $SS > 1.5$ are inactive (Bull and McFadden 1977). In the present study, the minimum value of the *SS* index is 1.114 for basin 10 and the maximum value is 2.102 for basin 9. The values are classified into three classes (Taesiri et al., 2020), i.e., Class 1 (1.114 – 1.171), Class 2 (1.172 – 1.450), and Class 3 (1.451 – 2.102) and spatially distributed (Fig. 10j).

Table 2 Geomorphic indices parameters.

Basin no	*Sl*	*Vfh*	*Hi*	*Af*	*BS*	*T*	*BE*	*SS*
1	270.94	8.54	0.09	19.15	3.08	0.41	0.49	1.17
2	119.71	0.90	0.21	17.33	1.76	0.44	0.48	1.30
3	121.17	1.15	0.13	26.68	1.63	0.54	0.66	1.41
4	62.58	0.70	0.29	13.96	1.49	0.24	0.65	1.12
5	85.32	0.90	0.16	0.14	1.58	0.08	0.68	1.45
6	190.84	1.61	0.09	11.83	2.53	0.41	0.50	1.22
7	172.87	0.26	0.16	3.40	2.65	0.32	0.58	1.31

8	624.21	4.90	0.16	9.81	1.21	0.27	0.68	1.92
9	466.87	1.41	0.00	16.39	2.01	0.19	0.61	2.10
10	179.31	0.66	0.07	12.91	2.23	0.33	0.67	1.11

395

396 **3.3. Indices of relative active tectonics (IRAT)**

397 In the present study, the morphometric indices consisting of linear and areal parameters and
398 the eight geomorphic indices are categorized into different classes and their average values are
399 considered for the evaluation of IRAT (Indices of relative active tectonics) (El Hamdouni et
400 al., 2008). The equation used for the calculation of IRAT is given as

401 $$\text{IRAT} = (\text{Avg Geo} + \text{Avg\_}Ln + \text{Avg } Al)/n$$

402 where Avg Geo, Avg_*Ln*, and Avg *Al* are average values of geomorphic indices, linear and
403 areal parameters class respectively and *n* denotes the number of parameters.

404 Table 3 Classes of Morphometric Indices.

Basin no	Linear Parameters			Areal Parameters					
	Br	*Lr*	*Avg_Ln*	*Fs*	*Dd*	*Dt*	*CR*	*Ff*	*Avg Al*
1	2	2	2	2	1	1	1	1	1.2
2	3	2	2.5	3	1	3	1	1	1.8
3	2	3	2.5	3	1	3	2	3	2.4
4	3	1	2	2	2	3	1	2	2
5	1	1	1	2	2	2	3	3	2.4
6	2	3	2.5	2	1	1	1	1	1.2
7	3	2	2.5	1	3	3	3	2	2.4
8	1	3	2	2	3	2	2	3	2.4
9	1	3	2	2	3	2	2	2	2.2

10	3	2	2.5	1	3	2	3	3	2.4

405

406 Table 4 Classes of geomorphic indices and calculation of IRAT.

Basin no	*Sl*	*Vfh*	*Hi*	*Af*	*BS*	*T*	*BE*	*SS*	Avg Geo	Avg_ *Ln*	Avg *Al*	IRAT	Class
1	1	3	3	1	1	1	1	1	1.50	2	1.2	1.57	1
2	3	2	1	2	3	1	1	2	1.88	2.5	1.8	2.06	2
3	2	3	2	1	3	1	2	2	2.00	2.5	2.4	2.30	4
4	3	2	1	2	3	2	2	1	2.00	2	2	2.00	2
5	3	2	2	3	3	3	3	2	2.63	1	2.4	2.01	2
6	2	3	1	2	1	1	1	2	1.63	2.5	1.2	1.78	1
7	2	1	2	3	1	2	2	2	1.88	2.5	2.4	2.26	3
8	1	3	2	2	3	2	3	3	2.38	2	2.4	2.26	3
9	1	3	3	2	2	3	2	3	2.38	2	2.2	2.19	3
10	2	1	3	2	2	2	3	1	2.00	2.5	2.4	2.30	4

407

408 Finally, the values obtained for IRAT are further classified into four classes as Class 1,
409 Class 2, Class 3, and Class 4 representing very high, high, moderate, and low tectonic activity,
410 respectively (Hamdouni et al., 2008; Mahmood and Gloaguen, 2012; Anand and Pradhan,
411 2019; Taesiri et al., 2020). The lowest value of IRAT is 1.57 for Basin 1 and the highest value
412 is 2.30 for Basin 3 and 10. The four classes for IRAT obtained in this study are Class1 (1.57 –
413 1.80) for very high, Class 2 (1.81 – 2.06) for high, Class 3 (2.07 – 2.26) for moderate, and Class
414 4 (2.27 – 2.30) for low tectonic activity (Fig. 11a). Basin 1 and 6 falls under class I covering
415 an area about 47740 km^2, a total area of 2507 km^2 of basin 2, 4 and 5 lies in class 2, basin 7, 8

and 9 falls under class 3 and it is comprised of total area 17495 km^2 and class 4 consists of basin 3 and 10 of total area 2090 km^2 (Table 4).

3.4. Faults distribution

Assam region is characterized by the presence of many major faults like Dhubri fault, Dhansiri Kopili fault, Kalyani shear, Dauki fault, etc. These faults contribute to the tectonic activity of the Assam region, so with the help of line density toolbox in ArcGIS 10.5 fault density map of the study area is prepared (Fig.11b) line density mainly calculates the magnitude-per-unit area from polyline features that fall within a radius around each cell. The zones which show high fault density have many fractured zones and due to erosional processes, these areas will have smoother topography and more tilting of the basin in comparison with adjacent areas. It is found that the region of basins 1, 6, and 9 show high fault density as well as it falls under classes 1 and 2 of asymmetric and transverse topographic symmetry factor. Therefore, it correlates with the asymmetric factor and transverse topographic symmetry of the basins as well as with the IRAT distribution map which shows very high tectonic activity in basins 1 and 6 and moderate tectonic activity in basin 9.

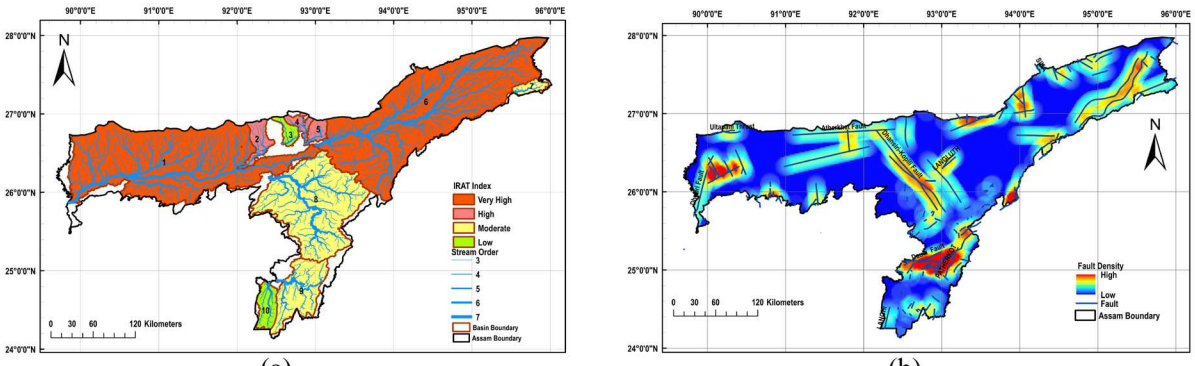

Fig. 11. Spatial distribution of (a) index of relative active tectonics (IRAT), and (b) fault density.

4. Discussion

435 The main aim of the study is the assessment, evaluation, and quantification of active
436 tectonics in the Assam region of India using the morphometric (two linear and five aerial
437 parameters) and eight geomorphic indices. Finally, an IRAT distribution map is prepared and
438 the entire study area is classified into four zones based on active tectonic. The results show that
439 the basins are having consistent relations with their geometry, structural discontinuity,
440 morphometric and geomorphic features.

441 **4.1. Linear and areal parameters**

442 In the present study, linear and areal parameters are evaluated on seven parameters for
443 the ten basins. The stream order of the basins is determined and it is found that the stream order
444 of the ten basins varies from 3rd order to 7th order (Fig. 5) (Strahler, 1952). With the increase
445 in the order of streams the number of segments decreases, for example, the stream of 7th order
446 will have less number of a stream than 6th order stream. The streams of lower order signify that
447 the basin area is highly dissected. The basins 1, 3, 5, 6, 8, and 9 which have higher value of
448 Bifurcation ratio (*Br*), major faults like Dhubri fault, Dhansiri Kopili fault, Kalyani shear,
449 Dauki fault, Main Frontal thrust, Main Central thrust, Main Boundary thrust, Naga thrust,
450 Bombdila fault, and Dudhnoi fault passes through it. Bifurcation ratio (*Br*) and stream length
451 ratio (*Lr*) are classified into three classes and it is found that 40,136 km^2 of the area of basin
452 falls under moderate tectonic activity zone, 29,009 km^2 of the area lies in the low tectonic
453 active zone and the high active tectonic zone constitutes 688 km^2 of area. Similarly, an average
454 of five areal parameters calculated in the study are classified into three zones, the area of the
455 basin which comes under high, moderate, and low active tectonic zones are 48,948 km^2, 4,800
456 km^{2,} and 16,086 km^2, respectively.

457 **4.2. Stream-length gradient index (*Sl*)**

458 The values of the *Sl* index and longitudinal profile of the river show an increasing trend
459 near the tectonically active zones. The values of stream-length gradient (*Sl*) index are

460 quantified for all ten basins of the study area and it is found that the majority of the basin area
461 falls under high to moderate zones i.e 39,525 km^2 is under high (Class 1) and 27,801 km^2 lies
462 in the moderate zone (Class 2). These two classes of basins have several major faults passing
463 through them or located in the vicinity of the basins. The total basin area of 2,507 km^2 is
464 classified as a low active tectonic zone (Class 3) with lower *Sl* values and it represents those
465 streams are flowing through those areas having strike-slip faults (Dehbozorgi *et al.,* 2010). The
466 higher value of *Sl* signifies tectonic control of the basins have variable lithological contrast and
467 thrusts (Sharma *et al.,* 2018) and tectonic activities are the cause of higher *Sl* index values
468 (Brookfield, 1998).

469 **4.3. Valley floor width to valley height Ratio (*Vfh*)**

470 The ratio of valley floor width to valley height (*Vfh*) identifies the presence of a tectonic
471 process or erosional process in a basin. Lower the value of *Vfh* signifies the dominance of
472 tectonic activity over the erosional process as result the shape of the valley is V-shaped for the
473 higher tectonic area and U-shaped for flat-floored valley or erosional process at bed level (Bull
474 and McFadden, 1977). It is found that the lowest value of *Vfh* 0.26 is obtained for basin 7 and
475 the highest value is 8.54 for basin 1, which indicates that the shape of basin 7 and basin 1 is
476 comprised of V- and U- shaped valley respectively. The value of *Vfh* is less than 1 for basins
477 2, 4, 5, 7, and 10 indicating a V-shaped valley with a young stage of basin development. The
478 *Vfh* value of basins 1, 3, 6, 8, and 9 is more than 1 and it denotes the predominance of erosional
479 processes due to which broad U-shaped valleys are formed. The majority of the area i.e., 65,286
480 km^2 of the area falls under U-shaped valleys or broad valleys and approximately 4,548 km^2 of
481 area represents a V-shaped valley.

482 **4.4. Hypsometric integral (*Hi*) and Hypsometric curve**

483 Hypsometric integral determines the total volume of the non-eroded basin and the
484 hypsometric curve represents the developmental stages of a basin (Hamdouni *et al.,* 2008). The

Hi values calculated for the basins ranges from 0.002 to 0.287 signifies concave and convex curve respectively. In the present study, the shape of the hypsometric curve is mainly an S-shaped curve for basins 2, 4, 5, and 7 representing moderately eroded regions (Pedrera *et al.,* 2009). Basins 1, 3, 6, 8, 9, and 10 show a concave curve which indicates that the regions are highly eroded and fractured due to the presence of structural discontinuity and according to the fault map of the study area major faults are present in these basins. According to the shape of the hypsometric curves obtained for all the ten basins, it is evident that the basins belong to matured to older stages. The total area of the basin belongs to class 1 is 1,818 km^2, Class 2 covers 14,652 km^2 of area and 53,363 km^2 of the area comes under Class 3. It is found that the majority of the basin area is highly eroded and indicates the presence of faults and fractures or structural discontinuity.

4.5. Asymmetric Factor (*Af*)

The asymmetry factor of all ten basins is calculated to determine the tilting of the basin due to tectonic activity. If the value of *Af* lies in the proximity of 50 then there will be no tilting and when the value of *Af* is greater than or less than 50 tilting of the basin will occur due to the influence of active tectonics (Ahmad et al., 2018). In the present study, Basin 1 and 3 belongs to Class 1 (19.15-26.68) covering an area of 23,293 km^2 and it is characterized as a highly tectonic zone due to the presence of major faults and thrusts like the Dhubri fault, Dhansiri Kopili fault, Main Frontal thrust, Main Boundary Thrust, and Dudhnoi fault. In Class 2 (11.18-19.14), the basin 2, 4, 6, 8, 9 and 10 falls under moderately active tectonic zones of 45,245 km^2 area, and basin 5 and 7 belong to Class 3 (< 11.17) i.e., a low active zone covering a total area of 1,295 km^2. It clearly states that the majority of the area falls under high to moderate active tectonic zones and it may be due to the presence of thrusts and faults passing through these basins.

4.6. Drainage Basin shape index (*BS*)

510 The shape of a basin is greatly influenced by the topographic evolution or tectonic
511 activity, so the basin shape index is calculated for the identification of tectonic activity of the
512 basin. Generally, elongated basins are dominant in tectonic active regions whereas circular
513 basins prevail in those regions which lack or exhibit low tectonic activity. The results of the
514 study show a strong correlation of the shape of the basin with the presence of tectonic features
515 like thrust, faults, or lineaments. The basin elongations are found in Basin 1, 6, and 7 and it
516 belongs to Class 1 (2.45 -3.08) i.e high tectonic activity, covering an area of 48,347 km^2. Major
517 faults and thrusts, namely, Dhubri fault, Dhansiri Kopili fault, Kalyani shear, Main Frontal
518 thrust, Main Central thrust, Main Boundary thrust, Bombdila fault, and Dudhnoi fault pass
519 through Class 1 basins. The moderate active tectonic basins in Class 2 (1.83 – 2.44), consisting
520 of Basin 9 and 10 having a total area of 5,622 km^2, belong to the Dauki fault and other structural
521 discontinuity. Class 3 (1.82 -1.21) indicates the basins having low tectonic activity and Basin
522 2,3,4,5 and 8 belong to this class with a total area of 15,864 km^2. It is evident from the results
523 that the majority of the basin area falls under high tectonic activity according to the basin shape
524 index.

525 **4.7. Transverse topographic symmetry (*T*)**

526 The values of transverse topographic symmetry (*T*) are evaluated for the measurement
527 of basin tilting due to tectonic activity and the value of $T = 0$ for symmetric basin and $T > 0$ for
528 the asymmetric basin (Cox, 1994). In this study, basin 1, 2, 3, and 6 are grouped under Class 1
529 (0.38-0.54) of high active tectonics (49,604 km^2 area), Basin 4, 7, 8 and 10 belongs to moderate
530 active tectonic zones (15,351 km^2 area) i.e., Class 2 (0.23 – 0.37) and Class 3 (0.08 – 0.22)
531 covers Basin 5 and 9 of low tectonic activity (4,877 km^2 area).

532 **4.8. Basin Elongation ratio (*BE*)**

533 Basin elongation ratio indicates the recent tectonic activity of a drainage basin. Basins for
534 which *BE* values lie below 0.50 are considered as tectonically active areas, from 0.50 to 0.75

535 are slightly active, and greater than 0.75 are inactive tectonic areas (Bull and McFadden, 1977).
536 In the present study, all the ten basins fall under active to slightly active class as the value
537 ranges from 0.477 to 0.684. Basin 1, 2, and 6 are represented as high tectonic active areas i.e.,
538 Class 1 (0.477 – 0.502), and its total area is 48,948 km^2, Class 2 (0.503 – 0.664) signifies a
539 moderately active zone consisting of Basin 3, 4, 7 and 9 with an area of approximately 6,063
540 km^2. Basin 8 and 10 belongs to Class 3 (0.665 – 0.684) contributing 14,133 km^2 area.

541 **4.9. Stream Sinuosity (*SS*)**

542 Stream sinuosity index is also used as a proxy indicator for the assessment of tectonic
543 activity. The high value of *SS* signifies a tectonically stable river basin and the low value
544 represents active basin area. In the present study, the range of the *SS* index varies from 1.11 to
545 2.10. Basin 1,4 and 10 corresponds to low *SS* value and therefore falls under Class 1 (1.11 –
546 1.17) of high tectonic zone (24,681 km^2 area), basin 2,3,5,6 and 7 classified as moderate active
547 zone (28,264 km^2 area) i.e., Class 2 (1.18 – 1.45) and Class 3 (1.46 – 2.10) comprised of Basin
548 8 and 9 revealing low active zone (16,888 km^2 area). According to the *SS* index value, the
549 majority of the area falls under the moderate tectonic activity zone category.

550 **4.10. Indices of relative active tectonics (IRAT)**

551 Previously, many studies have been performed on the assessment of relative tectonics
552 based on geomorphic or morphotectonics parameters for a small stretch of a river basin,
553 mountain front, smaller seismically active area, valleys of smaller area (Ahmad et., 2018;
554 Anand and Pradhan, 2019; Bhat et al., 2020; Bhattacharjee and Mohanty, 2020; Taesiri et al.,
555 2020 The present study is an attempt to investigate the spatial distribution of relative tectonics
556 in Assam region (78,438 km^2) by the application of geomorphic and morphometric indices on
557 ten delineated basins (total area 69,834 km^2). The average values of classes of two linear, five
558 areal, and eight geomorphic indices are calculated to obtain IRAT (Table 4). The values of

559 IRAT are classified into four classes as very high (Class 1), high (Class 2), moderate (Class 3),
560 and low (Class 4) based on relative active tectonics (Fig. 11a) (Hamdouni et al., 2008).
561 The minimum and maximum values of IRAT obtained for the study area are 1.57 and
562 2.30 respectively. The IRAT class 1 covers Basin 1 and 6 with a total area of 47,740 km^2, basin
563 2,4 and 5 lies in class 2 covering an area equal to 2,507 km^2, class 3 consists of basin 7, 8 and
564 9 of 17,495 km^2 in area and class 4 consists of basin 3 and 10 of total area 2090 km^2. The
565 present study area lies in the North-Eastern Himalayas and numerous studies have been
566 conducted for different parts of the Himalayan region and its adjacent areas by the combined
567 approach of two or more geomorphic indices to assess the relative tectonic in seismically active
568 regions (Topal 2018; Anand and Pradhan 2019; Bahrami et al., 2020). A morphotectonic study
569 conducted on tectonically active area NW Pakistan and NE Afghanistan, situated at the junction
570 of Hindu Kush-Karakorum-Himalayas shows that the IRAT values range from 1.0 to 2.33
571 (Mahmood and Gloaguen, 2012). The geomorphic study conducted for Alborz province,
572 located at the southern part of the Alborz Mountains (part of the Alps-Himalayan) shows that
573 it is one of the seismic tectonic active areas with IRAT value ranging from 1.0 to 2.58. (Taesiri
574 et al., 2020). The relative active tectonic assessment of the upper Ganga basin shows that the
575 landform is greatly affected by neotectonic activity with IRAT values ranging from 1.50 to
576 2.38 (Anand and Pradhan, 2019).
577 In this study, Class 1 (Basin 1 and 6) and Class 2 (Basin 2, 4 and 5) of IRAT mainly lie
578 along Dhubri fault, Dhansiri Kopili fault, Kalyani shear, Main Frontal thrust, Main Central
579 thrust, Main Boundary thrust, Bombdila fault, and Dudhnoi fault. Basins of these two IRAT
580 classes show the presence of neotectonic movements with high to a moderate value of stream
581 length gradients, asymmetry valleys, elongated basins deviation of streams from the midline of
582 the basins, stream sinuosity, and hypsometric integral. The basins of classes 1 and 2 represent
583 mostly U-shaped valleys with moderate to low valley floor width to height ratio index.

584 Very high to high IRAT values are along the mountain front, extending from west to
585 east of the study area and low to moderate IRAT values are found in central Assam and Barak
586 valley. it also reveals that the tectonic activity of the region is not uniformly distributed which
587 indicates the presence of a complex tectonic framework.

588 **5. Conclusion**

589 A GIS-based study of morphometric and geomorphic indices can be proved as useful
590 tools in the evaluation or assessment of active tectonics of a region. The morphometric and
591 geomorphic anomalies of an area can be studied by the application of these indices which are
592 calculated from remote sensing data i.e. DEM data and GIS tool. The Assam region falls under
593 seismic zone V with many major active faults and it had experienced great earthquakes in the
594 past. The complex tectonic and geological framework of the Assam region makes it susceptible
595 to seismic hazards. So, the method adopted in the present study is highly suitable for the
596 analysis of active tectonic of the Assam region. The drainage network for the study area is
597 derived from the DEM data of 30 m resolution and with the help of drainage data,
598 morphometric indices (two linear and five areal parameters) and eight geomorphic indices are
599 calculated for the ten delineated basins. Each index is classified into three active tectonic
600 classes ranging from high (Class 1) to low (Class 3) and Index of relative active tectonics
601 (IRAT) is evaluated by taking the average class value of linear, aerial, and geomorphic indices
602 further grouped into four tectonic activity classes (from very high to low active tectonics).

603 Spatial distribution of IRAT shows a strong correlation with the structural discontinuity
604 of the study area. The majority of the area falls under a very high to moderate active tectonic
605 zone except for Basin 3 and 10 lie in the low tectonic activity zone. Basin 1 and 6 lie in a very
606 high active tectonic zone with the presence of faults like Dhubri fault, Dhansiri Kopili fault,
607 Kalyani shear, Main Frontal thrust, Main Central thrust, Main Boundary thrust, Bombdila fault,
608 and Dudhnoi fault. Fault distribution map also supports the variation of IRAT in the study area

and it correlates with asymmetric factor and transverse topographic symmetry of the basins. It is evident from the results that morphometric indices (linear and areal parameters) have greatly influenced the tectonics of the study area as major faults and thrust like Dhubri fault, Dhansiri Kopili fault, Kalyani shear, Dauki fault, Main Frontal thrust, Main Central thrust, Main Boundary thrust, Naga thrust, Bombdila fault, and Dudhnoi fault passes through the basins. The *Vfh* indicates that the majority of the basin is U-shaped with the dominance of erosional processes. According to the values of asymmetric factor, it is found that most of the basins have structural discontinuity and influence of tectonic features like major faults and thrusts. Similarly, *Sl*, *Hi*, *Af*, *BS*, and *T* show higher values in those basins where major faults and thrusts are present. Lower values of *BE* and *SS* are also considered as determining factors for the presence of active tectonics in the study area. The present study will help in determining the change of topography of the landform with the evolution of time and its influence on the occurrence of natural hazards like earthquakes, landslides, floods, etc. This study will also help in the identification of the hazard-prone area to have well-defined disaster management and mitigation policies and measures.

CRediT authorship contribution statement

Laxmi Gupta: Methodology, Formal analysis, Software, Resources, Investigation, Data curation, Validation, Visualization, Writing - Original Draft. **Navdeep Agrawal:** Data curation, Validation, Writing - Original Draft. **Jagabandhu Dixit:** Conceptualization, Methodology, Software, Resources, Supervision, Project administration, Writing - Review & Editing. **Subashisa Dutta:** Writing - Review & Editing.

Declaration of interests

The authors declare that they have no known competing financial interests or personal relationships that could have appeared to influence the work reported in this paper.

633 **References**

634 1. Ahmad, S., Alam, A., Ahmad, B., Afzal, A., Bhat, M.I., Bhat, M.S., Ahmad, H.F. and
635 Tectonics and Natural Hazards Research Group, 2018. Tectono-geomorphic indices of the
636 Erin basin, NE Kashmir valley, India. *Journal of Asian Earth Sciences*, *151*, pp.16-30.
637 2. Alizadeh, A., Moghadam, H.H. and Seraj, M., 2020. DEM-derived geomorphic indices for
638 assessment of tectonic activity at the Dara anticlinal oil structure within the Zagros fold-
639 thrust belt, southwestern Iran. *Arabian Journal of Geosciences*, *13*(4), pp.1-13.
640 3. Anand, A.K. and Pradhan, S.P., 2019. Assessment of active tectonics from geomorphic
641 indices and morphometric parameters in part of Ganga basin. *Journal of Mountain*
642 *Science*, *16*(8), pp.1943-1961.
643 4. Bahrami, S., Capolongo, D. and Mofrad, M.R., 2020. Morphometry of drainage basins and
644 stream networks as an indicator of active fold growth (Gorm anticline, Fars Province,
645 Iran). *Geomorphology*, *355*, p.107086.
646 5. Bahuguna, A. and Sil, A., 2020. Comprehensive seismicity, seismic sources and seismic
647 hazard assessment of Assam, North East India. *Journal of Earthquake Engineering*, *24*(2),
648 pp.254-297.
649 6. Bhat, M.A., Dar, T. and Bali, B.S., 2020. Morphotectonic analysis of Aripal Basin in the
650 North-Western Himalayas (India): An evaluation of tectonics derived from geomorphic
651 indices. *Quaternary International*, *568*, pp.103-115.
652 7. Bhattacharjee, N. and Mohanty, S.P., 2020. GIS-based approach for the measurement of
653 variability in tectonomorphic signatures using DEM's data: a case study from the Habo
654 Dome in the Kachchh area, India. *Environmental Earth Sciences*, *79*(18), pp.1-26.
655 8. Bhukosh- Geological Survey of India URL:
656 https://bhukosh.gsi.gov.in/Bhukosh/MapViewer.aspx (Last assessed: 20 May 2021).

9. Biswas, M. and Paul, A., 2021. Application of geomorphic indices to Address the foreland Himalayan tectonics and landform deformation-Matiali-Chalsa-Baradighi recess, West Bengal, India. *Quaternary International*, *585*, pp.3-14.
10. Bull, W.B., and McFadden, L.D., 1977. Tectonic geomorphology north and south of the Garlock fault, California. In: Doehring, D.O. (Ed.), *Geomorphology in Arid Regions.* Proceedings of the Eighth Annual Geomorphology Symposium. State University of New York, Binghamton, pp. 115-138.
11. Catherine, J.K., 2004. A preliminary assessment of internal deformation in the Indian Plate from GPS measurements. *Journal of Asian Earth Sciences*, 23(4), pp.461-465.
12. Cheng, W., Wang, N., Zhao, M. and Zhao, S., 2016. Relative tectonics and debris flow hazards in the Beijing Mountain area from DEM-derived geomorphic indices and drainage analysis. *Geomorphology*, *257*, pp.134-142.
13. Cox, R.T., 1994. Analysis of drainage-basin symmetry as a rapid technique to identify areas of possible Quaternary tilt-block tectonics: An example from the Mississippi Embayment. *Geological Society of America Bulletin*, 106(5), pp.571-581.
14. Das, J.D., Shujat, Y. and Saraf, A.K., 2011. Spatial technologies in deriving the morphotectonic characteristics of tectonically active Western Tripura Region, Northeast India. *Journal of the Indian Society of Remote Sensing*, 39(2), pp.249-258.
15. Dawit, M., Olika, B.D., Muluneh, F.B., Leta, O.T. and Dinka, M.O., 2020. Assessment of Surface Irrigation Potential of the Dhidhessa River Basin, Ethiopia. *Hydrology*, *7*(3), p.68.
16. Daxberger, H., Dalumpines, R., Scott, D.M. and Riller, U., 2014. The ValleyMorph Tool: An automated extraction tool for transverse topographic symmetry (T-) factor and valley width to valley height (Vf-) ratio. *Computers & Geosciences*, *70*, pp.154-163.

17. Devi, R.M., 2008. Geomorphic appraisals of active tectonics associated with uplift of the Gohpur–Ganga section in Itanagar, Arunachal Pradesh, India. *Geomorphology,* 99(1-4), pp.76-89.

18. Divyadarshini, A. and Singh, V., 2019. Investigating topographic metrics to decipher structural model and morphotectonic evolution of the Frontal Siwalik Ranges, Central Himalaya, Nepal. *Geomorphology*, *337*, pp.31-52.

19. Dixit, J., Raghukanth, S.T.G., Dash, S.K., 2016. Spatial Distribution of Seismic Site Coefficients for Guwahati City. In *Geostatistical and Geospatial Approaches for the Characterization of Natural Resources in the Environment,* Springer: Cham, Switzerland, pp. 533–537.

20. El Hamdouni, R., Irigaray, C., Fernández, T., Chacón, J. and Keller, E.A., 2008. Assessment of relative active tectonics, southwest border of the Sierra Nevada (southern Spain). *Geomorphology*, *96*(1-2), pp.150-173.

21. Ghosh, B., Mukhopadhyay, S., Morishita, T., Tamura, A., Arai, S., Bandyopadhyay, D., Chattopadhaya, S. and Ovung, T.N., 2018. Diversity and evolution of suboceanic mantle: constraints from Neotethyan ophiolites at the eastern margin of the Indian plate. *Journal of Asian Earth Sciences*, *160*, pp.67-77.

22. Gu, Z., Shi, C. and Peng, J., 2019. Evolutionary dynamics of the main-stem longitudinal profiles of ten kongdui basins within Inner Mongolia, China. *Journal of Geographical Sciences*, *29*(3), pp.417-431.

23. Hack, J.T., 1973. Stream-profile analysis and stream-gradient index. *Journal of Research of the US Geological Survey*, *1*(4), pp.421-429.

24. Hare, P.W. and Gardner, T.W., 1985. Geomorphic indicators of vertical neotectonism along converging plate margins, Nicoya Peninsula, Costa Rica. *Tectonic Geomorphology*, *4*, pp.75-104.

25. Horton, R.E., 1945. Erosional development of streams and their drainage basins; hydrophysical approach to quantitative morphology. Geological Society of America Bulletin, 56(3), pp.275-370.
26. ISC, International Seismological Centre, ISC-GEM Earthquake Catalogue 2021, URL: https://doi.org/10.31905/d808b825 (last accessed: 20 May 2021).
27. Khan, S., Fryirs, K.A. and Shumack, S., 2021. Semi-automating the calculation of catchment scale geomorphic controls on river diversity using publically available datasets. *Catena*, *203*, p.105354.
28. Koukouvelas, I.K., Zygouri, V., Nikolakopoulos, K. and Verroios, S., 2018. Treatise on the tectonic geomorphology of active faults: The significance of using a universal digital elevation model. *Journal of Structural Geology*, *116*, pp.241-252.
29. Latrubesse, E.M., 2008. Patterns of anabranching channels: The ultimate end-member adjustment of mega rivers. *Geomorphology*, *101*(1-2), pp.130-145.
30. Longkumer, L., Luirei, K., Moiya, J.N. and Thong, G.T., 2019. Morphotectonics and neotectonic activity of the Schuppen Belt of Mokokchung, Nagaland, India. *Journal of Asian Earth Sciences*, 170, pp.138-154.
31. Mahmood, S.A. and Gloaguen, R., 2012. Appraisal of active tectonics in Hindu Kush: Insights from DEM derived geomorphic indices and drainage analysis. *Geoscience Frontiers*, *3*(4), pp.407-428.
32. Mishra, M.N., 2019. Active tectonic deformation of the Shillong plateau, India: Inferences from river profiles and stream gradients. *Journal of Asian Earth Sciences*, 181, p.103904.
33. Mueller, J.E., 1968. An introduction to the hydraulic and topographic sinuosity indexes. *Annals of the Association of American Geographers*, *58*(2), pp.371-385.
34. Panda, D., Kundu, B. and Santosh, M., 2018. Oblique convergence and strain partitioning in the outer deformation front of NE Himalaya. *Scientific Reports*, *8*(1), pp.1-9.

730 35. Pei, Y., Qiu, H., Hu, S., Yang, D., Zhang, Y., Ma, S. and Cao, M., 2021. Appraisal of
731 tectonic-geomorphic features in the Hindu Kush-Himalayas. *Earth and Space Science*,
732 p.e2020EA001386.
733 36. Raghukanth, S., Dixit, J., Dash, S., 2011. Ground motion for scenario earthquakes at
734 Guwahati city. *Acta Geod. Geophys. Hung*., 46, 326–346.
735 37. Raj, R., 2012. Active tectonics of NE Gujarat (India) by morphometric and
736 morphostructural studies of Vatrak River basin. *Journal of Asian Earth Sciences*, *50*,
737 pp.66-78.
738 38. Ramírez-Herrera, M.T., 1998. Geomorphic assessment of active tectonics in the Acambay
739 Graben, Mexican volcanic belt. Earth Surface Processes and Landforms: *The Journal of*
740 *the British Geomorphological Group*, 23(4), pp.317-332.
741 39. Rodríguez, M.O.C., Barba, D.C. and Escribano, D.N., 2017. Morphotectonic study of the
742 Greater Antilles. *Geotectonics*, 51(1), pp.89-104.
743 40. Saber, R., Caglayan, A. and Isik, V., 2018. Relative tectonic activity assessment and
744 kinematic analysis of the North Bozgush fault Zone, NW Iran. *Journal of Asian Earth*
745 *Sciences*, 164, pp.219-236.
746 41. Saber, R., Isik, V. and Caglayan, A., 2020. Tectonic geomorphology of the Aras drainage
747 basin (NW Iran): Implications for the recent activity of the Aras fault zone. *Geological*
748 *Journal*, *55*(7), pp.5022-5048.
749 42. Sarp, G. and Duzgun, S., 2015. Morphometric evaluation of the Afşin-Elbistan lignite basin
750 using kernel density estimation and Getis-Ord's statistics of DEM-derived indices, SE
751 Turkey. *Journal of Asian Earth Sciences*, *111*, pp.819-826.
752 43. Schumm, S.A., 1956. Evolution of drainage systems and slopes in badlands at Perth
753 Amboy, New Jersey. *Geological Society of America Bulletin*, *67*(5), pp.597-646.

754 44. Sharma, S. and Sarma, J.N., 2017. Application of drainage basin morphotectonic analysis
755 for assessment of tectonic activities over two regional structures of northeast India. *Journal*
756 *of the Geological Society of India*, *89*(3), pp.271-280.
757 45. Shukla, D.P., Dubey, C.S., Ningreichon, A.S., Singh, R.P., Mishra, B.K. and Singh, S.K.,
758 2014. GIS-based morpho-tectonic studies of Alaknanda river basin: a precursor for hazard
759 zonation. *Natural Hazards*, *71*(3), pp.1433-1452.
760 46. Silalahia, F.E.S. and Hidayatb, F., 2019. Modelbuilder and Unit Hydrograph for Flood
761 Prediction and Watershed Flow Direction Determination at the West Branch of the Little
762 River, Stowe, Lamoille County, Vermont, USA. *Geoplanning: Journal of Geomatics and*
763 *Planning*, *6*(2), pp.89-98.
764 47. Silva, P.G., Goy, J.L., Zazo, C. and Bardajı, T., 2003. Fault-generated mountain fronts in
765 southeast Spain: geomorphologic assessment of tectonic and seismic activity.
766 *Geomorphology*, 50(1-3), pp.203-225.
767 48. Singh, Y. and Chaudhri, A.R., 2020. Morphotectonic Study of Frontal Siwalik Hills, near
768 Gandhiri, Kangra, Himachal Pradesh, India. *Open Journal of Geology*, 10(04), p.280.
769 49. Sreedevi, P.D., Subrahmanyam, K. and Ahmed, S., 2005. The significance of
770 morphometric analysis for obtaining groundwater potential zones in a structurally
771 controlled terrain. *Environmental Geology*, *47*(3), pp.412-420.
772 50. Strahler, A.N., 1952. Hypsometric (area-altitude) analysis of erosional
773 topography. *Geological Society of America Bulletin*, *63*(11), pp.1117-1142.
774 51. Taesiri, V., Pourkermani, M., Sorbi, A., Almasian, M. and Arian, M., 2020.
775 Morphotectonics of Alborz Province (Iran): A Case Study Using GIS
776 Method. *Geotectonics*, *54*(5), pp.691-704.
777 52. Topal, S., 2018. Quantitative analysis of relative tectonic activity in the Acıgöl fault, SW
778 Turkey. *Arabian Journal of Geosciences*, *11*(9), pp.1-10.

53. USGS EARTH EXPLORER URL: https://earthexplorer.usgs.gov/ (last accessed: 22 May 2021).

54. USGS NEIC. US Geological Survey National Earthquake Information Centre 2021, URL: http://earthquake.usgs.gov/earthquakes (last accessed: 20 May 2021).

55. Zhang, T., Fan, S., Chen, S., Li, S. and Lu, Y., 2019. Geomorphic evolution and neotectonics of the Qianhe River Basin on the southwest margin of the Ordos Block, North China. *Journal of Asian Earth Sciences*, 176, pp.184-195.